

300
3/12/81

1.5

②

Dr. 2468

SERI/PR-9192-1-T2

MASTER

THIN FILM POLYCRYSTALLINE SILICON SOLAR CELLS

Second Technical Progress Report for Period July 16—October 15, 1980

October 1980

Work Performed Under Contract No. AC02-77CH00178

Poly Solar Incorporated
Garland, Texas

7/15/80
DT/15-23



U.S. Department of Energy



Solar Energy

DISCLAIMER

This report was prepared as an account of work sponsored by an agency of the United States Government. Neither the United States Government nor any agency Thereof, nor any of their employees, makes any warranty, express or implied, or assumes any legal liability or responsibility for the accuracy, completeness, or usefulness of any information, apparatus, product, or process disclosed, or represents that its use would not infringe privately owned rights. Reference herein to any specific commercial product, process, or service by trade name, trademark, manufacturer, or otherwise does not necessarily constitute or imply its endorsement, recommendation, or favoring by the United States Government or any agency thereof. The views and opinions of authors expressed herein do not necessarily state or reflect those of the United States Government or any agency thereof.

DISCLAIMER

Portions of this document may be illegible in electronic image products. Images are produced from the best available original document.

DISCLAIMER

"This book was prepared as an account of work sponsored by an agency of the United States Government. Neither the United States Government nor any agency thereof, nor any of their employees, makes any warranty, express or implied, or assumes any legal liability or responsibility for the accuracy, completeness, or usefulness of any information, apparatus, product, or process disclosed, or represents that its use would not infringe privately owned rights. Reference herein to any specific commercial product, process, or service by trade name, trademark, manufacturer, or otherwise, does not necessarily constitute or imply its endorsement, recommendation, or favoring by the United States Government or any agency thereof. The views and opinions of authors expressed herein do not necessarily state or reflect those of the United States Government or any agency thereof."

This report has been reproduced directly from the best available copy.

Available from the National Technical Information Service, U. S. Department of Commerce, Springfield, Virginia 22161.

Price: Printed Copy A03
Microfiche A01

THIN FILM POLYCRYSTALLINE SILICON SOLAR CELLS

Second Technical Progress Report

Covering the Period July 16, 1980 to October 15, 1980

Prepared under SERI Subcontract XZ-φ-9192-1

by

Poly Solar Incorporated
2701 National Drive
Garland, Texas 75041

October, 1980

CONTENTS

List of Illustrations	iii
List of Tables	iv
Summary	1
I. Introduction	2
II. Purification of Metallurgical Silicon	3
III. Metallurgical Silicon Substrates	7
IV. Epitaxial Silicon Films on Metallurgical Silicon Substrates	15
V. Thin Film Silicon Solar Cells	18
VI. Plan for the Next Period	25

List of Illustrations

Figure 1	A typical positive SIMS spectrum of metallurgical silicon substrate prepared from aqua regia extracted metallurgical silicon by unidirectional solidification on graphite.	8
Figure 2	Positive SIMS spectrum of commercial metallurgical grade silicon.	9
Figure 3	Concentration profile of major impurities along the length of a metallurgical silicon substrate.	12
Figure 4	Current-voltage characteristics of a 37 cm^2 area polycrystalline thin film silicon solar cell under illumination with GE ELH quartz-halogen lamps equivalent to AM1 conditions.	21
Figure 5	Current-voltage characteristics of a 60 cm^2 area polycrystalline thin film silicon solar cell under illumination with GE ELH quartz-halogen lamps equivalent to AM1 conditions.	22
Figure 6	Short-circuit current and open circuit voltage relations of the thin film silicon solar cell shown in Fig. 4.	23
Figure 7	Spectral response of the thin film silicon solar cell shown in Figure 4.	24

List of Tables

Table I	Concentration of metallic impurities (mg/l) in the successive aqua regia extracts after refluxing with metallurgical silicon.	5
Table II	Concentration of aluminum and iron (ppma) in as-received metallurgical silicon and metallurgical silicon purified by aqua-regia extraction under different conditions.	6
Table III	Semiquantitative analysis of metallurgical silicon and unidirectionally solidified partially-purified metallurgical silicon substrates by secondary ion mass spectroscopy (average of 32 sample points for metallurgical silicon and average of 24 sample points for silicon substrates).	11
Table IV	Effect of heat treatment on impurity distribution in partially purified metallurgical silicon substrate.	13
Table V	Effect of heat treatment on impurity distribution in epitaxial silicon layer on metallurgical silicon substrate.	16

Summary

This is the Second Technical Progress Report of a research program "Thin Films Polycrystalline Silicon Solar Cells" supported by the Solar Energy Research Institute under Subcontract No. XZ-φ-9192-1. The objectives of this contract are to fabricate large area thin film silicon solar cells with AM1 efficiency of 10% or greater with good reproducibility and good yield and to assess the feasibility of implementing this process for manufacturing solar cells at a cost of \$300/kWe.

Efforts during the past quarter have been directed to the purification of metallurgical silicon, the preparation and characterization of substrates and epitaxial silicon layers, and the fabrication and characterization of solar cells. The partial purification of metallurgical silicon by extraction with aqua regia has been further investigated in detail, and the resulting silicon was analyzed by the atomic absorption technique. The unidirectional solidification of aqua regia-extracted metallurgical silicon on graphite was used for the preparation of substrates, and the impurity distribution in the substrate was determined and compared with the impurity content in metallurgical silicon. The effects of heat treatment on the impurity distribution in the substrate and in the epitaxial layer have also been investigated.

Large area (30-60 cm²) solar cells have been prepared from aqua regia-extracted metallurgical silicon substrates by depositing a p-n junction structure using the thermal reduction of trichlorosilane containing appropriate dopants. Chemically deposited tin-dioxide films were used as antireflection coatings. The AM1 efficiencies are about 9% for cells of 30-35 cm² area. Larger area, 60 cm², thin film solar cells have been fabricated for the first time, and their AM1 efficiencies are slightly higher than 8%. The spectral response, minority carrier diffusion length, and I_{sc} - V_{oc} relation in a number of solar cells have been measured.

I. Introduction

This is the Second Technical Progress Report of a research program "Thin Films Polycrystalline Silicon Solar Cells" supported by the Solar Energy Research Institute under Subcontract No. XZ-Φ-9192-1. The objectives of this contract are to fabricate large area thin film silicon solar cells with AM1 efficiency of 10% or greater with good reproducibility and good yield and to assess the feasibility of implementing this process for manufacturing solar cell at a cost of \$300/kWe.

The principal approach used in this work is the deposition of a silicon film of controlled thickness and dopant concentration on a partially purified metallurgical silicon substrate by the thermal reduction of trichlorosilane, the most economical process for the manufacture of polycrystalline silicon. Metallurgical silicon was selected as the substrate because of its crystal structure and low cost. During this reporting period, efforts were directed to (1) the purification of metallurgical silicon, (2) the preparation and characterization of metallurgical silicon substrates, and (3) the deposition and characterization of silicon solar cells on purified metallurgical silicon substrates. The experimental procedures and results are summarized in the following sections.

II. Purification of Metallurgical Silicon

The partial purification of pulverized metallurgical grade silicon by acid extraction has been continued. This technique is based on the assumption that a major portion of metallic impurities precipitates at grain boundaries during the solidification of metallurgical silicon melt in the manufacturing process. The prolonged treatment of pulverized material with acids can therefore dissolve these impurities. The use of aqua regia has been shown to be more effective than the use of hydrochloric acid or an equivolume mixture of nitric acid and sulfuric acid. The standard procedure developed at Poly Solar consists of refluxing about 1.5 kg of metallurgical silicon of 30-80 mesh size with 2.5 l of aqua regia for a total of 400 hrs; where the acid was replaced every 100 hrs. The resulting material was rinsed with water and dried.

Commercially available nitric acid and hydrochloric acid contain about 68% (weight) HNO_3 and 38% (weight) HCl , respectively. During the refluxing process, the reaction between nitric acid and hydrochloric acid yields nitrogen dioxide and chlorine which escape from the solution. Hydrogen chloride also vaporizes from the solution until its concentration is reduced to about 20% (weight), when the concentration of hydrochloric acid in solution remains constant (constant boiling hydrochloric acid). Thus, the rate of reaction between aqua regia and impurities in metallurgical silicon decreases with time due to the depletion of acids in the solution. Since the dissolution of metallic impurities in constant boiling hydrochloric acid has been shown to be slower than that in aqua regia, it was thought that the duration of refluxing might be decreased without reducing appreciably the extent of the dissolution of impurities. The impurity contents in the successive acid-extracts after different refluxing times, analyzed by the atomic

absorption technique, are summarized in Table I. In these experiments, 1.5 kg of pulverized metallurgical silicon and 2.5 l of aqua regia were refluxed for a prescribed duration, 24 or 100 hrs. The acid was replaced and the refluxing continued for the same duration, and this process was repeated two more times. It is apparent from Table I that during the first extraction, longer duration of refluxing removes more impurities. The impurity concentrations in the second extract after 24 hrs. refluxing are higher than those after 100 hr. refluxing due to the higher impurity content in metallurgical silicon after the first 24 hr. refluxing. The total amount of each impurity removed after the four refluxing periods increases with increasing duration of refluxing, and the use of 100 hr. refluxings is more effective. Also, aluminum, copper, manganese, vanadium, and titanium are more readily removed than iron and nickel, as indicated by the concentration of these impurities in the successive extracts. However, not all impurities which can be dissolved by aqua regia have been removed by the 400 hr. refluxing with acid changed every 100 hrs. Further improvements of the acid-extraction technique will be carried out.

The concentrations of aluminum and iron in metallurgical silicon after 2 - 24 hr, 4 - 24 hr, and 4 - 100 hr. refluxing with aqua regia were also analyzed by the atomic absorption technique. The results, as summarized in Table II, also suggest that acid-extraction is a slow process and that further improvements must be made for large scale applications.

Table I Concentration of Metallic Impurities (mg/liter) in the successive aqua regia extract after refluxing with metallurgical silicon.

Duration of refluxing, hrs.	First Extract		Second Extract		Third Extract		Fourth Extract		Total	
	24	100	24	100	24	100	24	100	24	100
Aluminum	470	670	25.4	14.2	2.1	4.1	0.80	3.1	498	691
Iron	860	1,430	136	135	120	76	102	112	1,218	1,753
Copper	10.2	13.8	0.53	0.31	0.31	0.33	0.25	0.24	11.3	14.7
Manganese	169	250	11.4	10.7	8.6	3.9	3.0	2.7	192	267
Nickel	5.0	35.6	12.3	10.6	14.5	11.7	11.4	11.2	43.2	69.1
Vanadium	0.9	3.1	0.2	0.3	0.1	0.2	0.1	0.1	1.3	3.7
Titanium	7.6	16.7	1.1	1.1	0.4	0.7	0.4	0.5	9.5	19

Table II Concentration of aluminum and iron (ppma) in as-received metallurgical silicon and metallurgical silicon purified by aqua-regia extraction under different conditions.

	Metallurgical Silicon	MG Si after 24 hr.refluxing	MG Si after 2 ⁴ hr.refluxing	MG Si after 4100 hr.refluxing
Al	610	400	350	320
Fe	1,500	750	570	350

III. Metallurgical Silicon Substrates

The pulverized metallurgical grade silicon purified by aqua-regia extraction was used for the preparation of substrates by unidirectional solidification on graphite. In this technique, purified metallurgical silicon is placed on a graphite plate of 7.5 cm x 28 cm area in a fused silica tube of 10.5 cm ID. Graphite is heated externally by an rf generator, and the spacings between the turns of the rf coil are adjusted to yield a unidirectional temperature gradient of 70°-100°C along the length of the specimen. The entire specimen was first heated at a temperature above the melting point of silicon, and the input power was reduced for the solidification to take place from one end of the specimen to the other. Since the solidification process initiates from the surface of the melt and proceeds inward, the random nucleation at the silicon-graphite interface has no effects on the grain structure of the surface region of the solidified material. The maximum rate of solidification is 1.5-2 cm/min; non-planar surfaces with ridges and valleys are obtained at higher rates. By controlling the thermal conditions to yield a planar solid-liquid interface, elongated crystallites of several centimeters length have been obtained.

To determine the impurity concentration and distribution in unidirectionally solidified metallurgical silicon substrates, a strip of about 2 cm width was cut along the length of a substrate, and this strip was further cut into twelve pieces of about 2 cm length each. The elemental analysis inside a grain of each sample was then carried out using the SIMS technique through the courtesy of Dr. Larry Kazmerski of SERI. A typical SIMS spectrum of the substrate is shown in Fig. 1, and a SIMS spectrum of as-received metallurgical silicon is shown in Fig. 2 for comparison. The data were obtained by using an oxygen jet (10^{-7} torr) on specimen surface to enhance secondary ion yields.

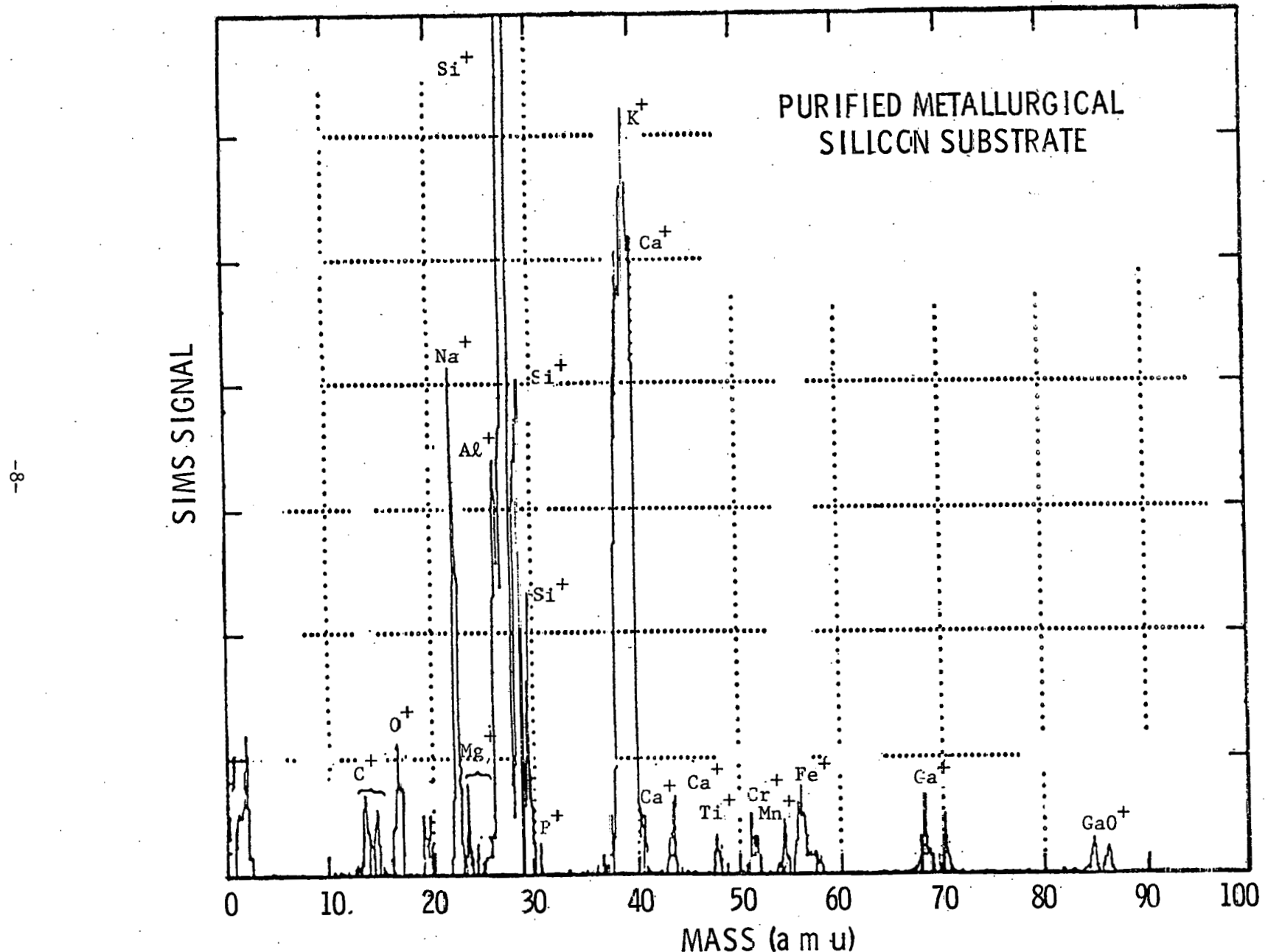


Figure 1 A typical positive SIMS spectrum of metallurgical silicon substrate prepared from aqua-regia extracted metallurgical silicon by unidirectional solidification on graphite.

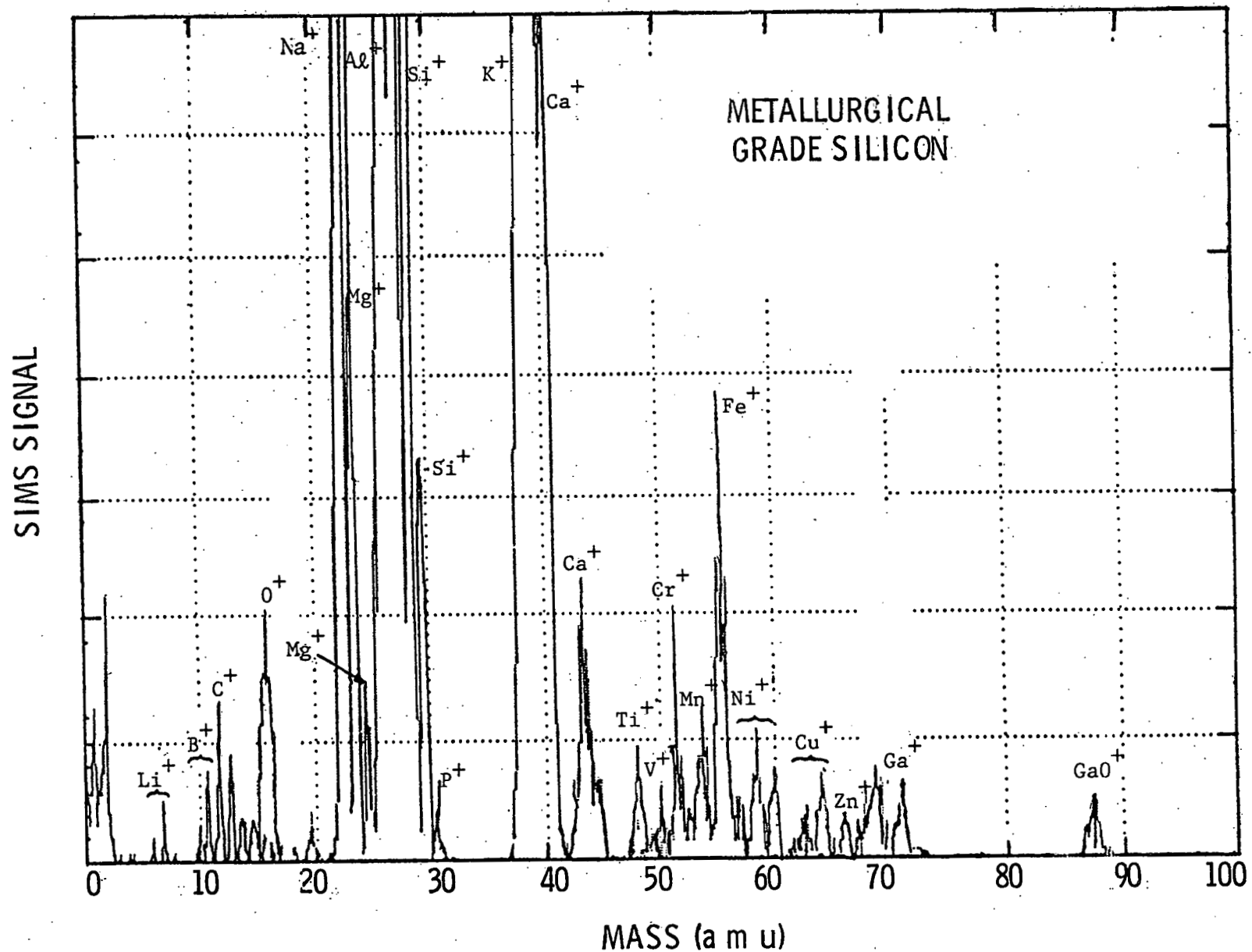


Figure 2 Positive SIMS spectrum of commercial metallurgical grade silicon.

It is apparent that the concentrations of sodium, magnesium, aluminum, calcium, titanium, vanadium, chromium, manganese, iron, nickel, cobalt, copper, and zinc in the substrate are significantly lower than those in metallurgical silicon.

The semi quantitative analysis of metallurgical grade silicon and metallurgical silicon substrates was carried out in detail using the SIMS technique. Thirty-two metallurgical silicon samples and twenty-four regions of metallurgical silicon substrates were analyzed. The average concentration of impurities in metallurgical grade silicon and metallurgical silicon substrates are summarized in Table III, where the peak intensity and relative atomic fraction of all detectable elements are given. The considerably reduced impurity concentration in the metallurgical silicon substrate is again apparent.

The concentration profile of most significant impurities along the length of the metallurgical silicon substrate was determined from the SIMS analysis of each 2 cm x 2 cm specimen described above. The results are shown in Fig.3. The concentrations of aluminum, iron, and chromium are essentially uniform throughout indicating negligible segregation during the solidification process.

Metallurgical silicon substrates were subjected to heat treatment in an inert atmosphere, such as helium, at 700°C for various durations. In all cases, the concentration of metallic impurities at grain boundaries was found to increase appreciably. An example is shown in Table IV where the relative atomic fractions of elements in the grains and grain boundaries of an as-recrystallized substrate and in the grains and grain boundaries of a heat-treated substrate (700°C, 12 hrs) are summarized. After heat treatment, the concentrations of titanium, iron, and zinc at the grain boundaries are significantly higher than those before heat treatment, and vanadium, cobalt, nickel, copper, and zinc are detected at the grain boundaries only after heat treatment. Thus, grain boundaries served as a sink for the precipitation of

Table III. Semiquantitative analysis of metallurgical silicon and unidirectionally solidified partially-purified metallurgical silicon substrates by secondary ion mass spectroscopy (average of 32 sample points for metallurgical silicon and average of 24 sample points for silicon substrates).

Y	Metallurgical-Grade Si			Substrate Si		
	$\langle I \rangle$	$\langle I/Y \rangle$	$\langle f_i \rangle$	$\langle I \rangle$	$\langle I/Y \rangle$	$\langle f_i \rangle$
Li	3.92	0.008	0.002	0.0002	-	-
B	0.35	0.011	0.031	0.004	-	-
C	1.10	0.036	0.032	0.004	0.03	0.027
Na	2.84	1.68	0.592	0.077	1.42	0.50
Mg	2.84	0.28	0.099	0.013	0.12	0.042
Al	3.73	2.14	0.573	0.074	1.80	0.483
Si	1.00	6.00	6.00	0.774	6.25	6.25
P	0.06	0.001	0.017	0.002	0.001	0.017
K	28.00	2.00	0.071	0.009	2.04	0.072
Ca	9.51	1.06	0.111	0.015	0.60	0.063
Ti	3.60	0.04	0.011	0.001	0.03	0.008
V	4.90	0.004	0.001	0.0001	-	-
Cr	6.10	0.40	0.066	0.009	0.07	0.012
Mn	3.27	0.026	0.008	0.001	0.02	0.006
Fe	1.90	0.140	0.074	0.010	0.03	0.016
Co	1.94	0.002	0.001	0.0001	-	-
Ni	1.50	0.011	0.007	0.001	-	-
Cu	1.13	0.011	0.009	0.001	-	-
Zn	0.18	0.006	0.033	0.004	-	-
Ga	9.40	0.008	0.001	0.0001	0.006	0.0006

Y = Sensitivity Factor

I = SIMS peak intensity

f_i = Atomic fraction $\{ = (I_i/Y_i)/ \sum_j (I_j/Y_j) \}$

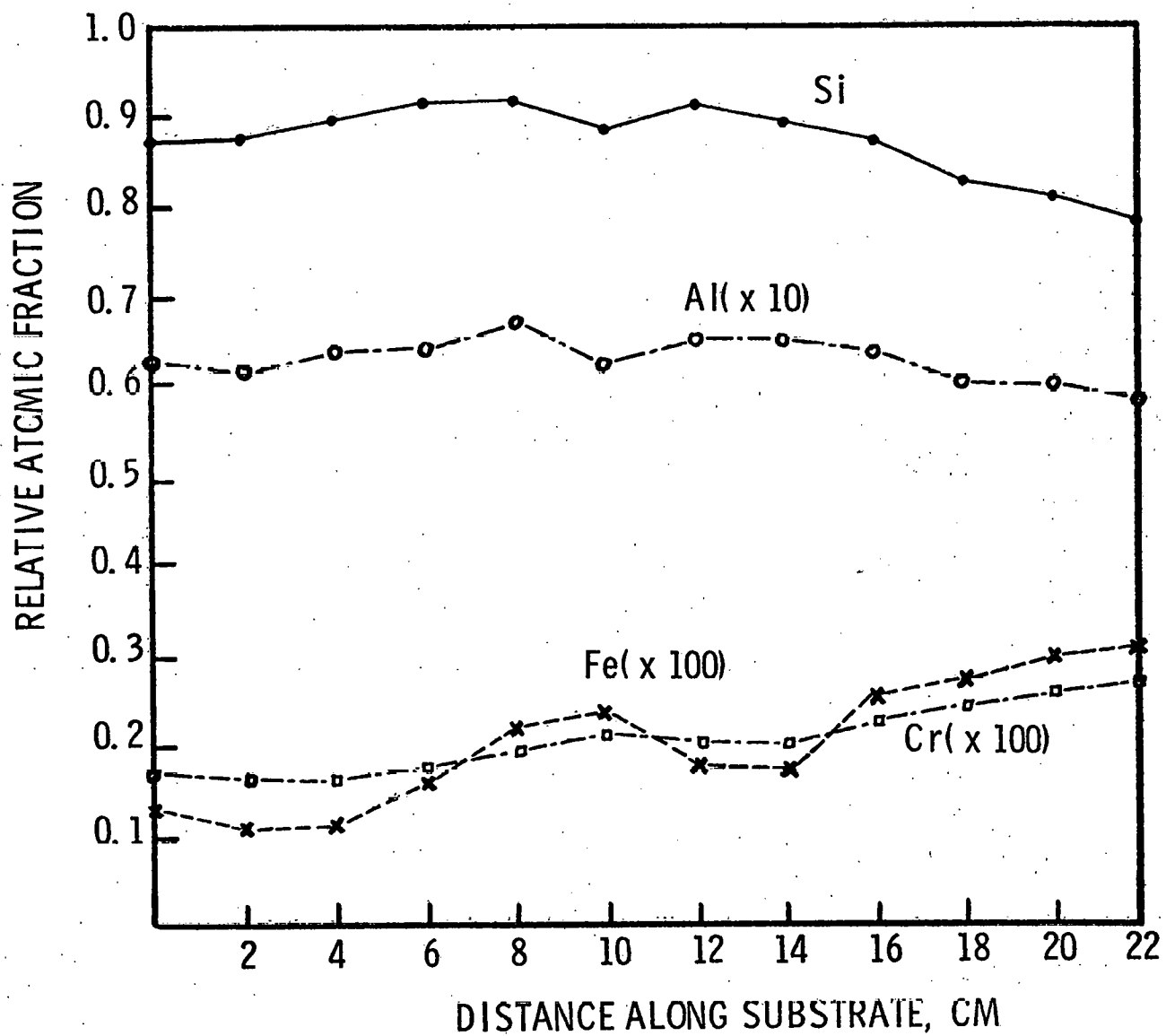


Figure 3 Concentration profile of major impurities along the length of a metallurgical silicon substrate.

Table IV Effect of heat treatment on impurity distribution in partially purified metallurgical silicon substrate.

Relative Atomic Fraction of Elements Deduced from SIMS Data

	As-Recrystallized Substrate		Substrate heated at 700°C for 12 hrs	
	Grain	Grain Boundary	Grain	Grain Boundary
B		0.002		0.006
C	0.004	0.006	0.003	0.0048
Na	0.067	0.07	0.062	0.069
Mg	0.006	0.01	0.006	0.010
Al	0.064	0.08	0.066	0.074
Si	0.834	0.80	0.840	0.80
P	0.002	0.003		0.002
K	0.010	0.01	0.010	0.01
Ca	0.008	0.01	0.013	0.011
Ti	0.001	0.001	0.0008	0.003
Cr	0.002	0.002	0.0001	0.002
Mn	0.0008	0.001		0.001
Fe	0.002	0.004		0.006
V				0.00005
Co				0.00007
Ni				0.0006
Cu				0.0001
Zn		0.0005		0.0015

metallic impurities, and the presence of grain boundaries may be considered as an advantage in using low purity silicon for solar cell purposes.

IV. Epitaxial Silicon Films on Metallurgical Silicon Substrates

Epitaxial silicon films have been deposited on metallurgical silicon substrates of 7.5 cm x 28 cm area by the thermal reduction of trichlorosilane with hydrogen. Since the substrate was prepared by the unidirectional solidification of partially purified metallurgical silicon on graphite, the graphite serves as the susceptor for the heating of the substrate. The substrate/graphite was placed in a fused silica tube of 10.5 cm ID and heated externally with an rf generator. The in-situ etching of the substrate with a hydrogen-hydrogen chloride mixture at 1200°C was used to remove 2-3 μm of silicon from the substrate surface. The deposition of silicon was then carried out at 1100°C. As the substrate is always p-type with a resistivity of 0.04 - 0.06 ohm-cm, p-type epitaxial layers of 0.2 - 0.5 ohm-cm resistivity were deposited routinely to determine their thickness and thickness uniformity, and resistivity and resistivity uniformity. In general, the thickness of the epitaxial film along the length of the specimen is uniform within 10%, and the resistivity is uniform within 15%. However, the p-type dopant, 25 ppm diborane in hydrogen, was found to degrade with time, and periodic measurements of the resistivity of epitaxial silicon films are essential.

The impurity concentration in p-type epitaxial films on metallurgical silicon substrates was also analyzed by Dr. Larry Kazmerski of SERI using the SIMS technique. The elemental analysis in the grains and grain boundaries of the epitaxial films was carried out. There is essentially no difference in impurity contents at both regions. Typical results are shown in Table V, where the relative atomic fraction of all detectable elements are summarized. A comparison of Table V with Table IV indicates considerably reduced concentrations of magnesium, aluminum, calcium, chromium, and manganese in the epitaxial layer, and titanium and iron are not detected in the epitaxial layer.

Table V Effect of heat treatment on impurity distribution in epitaxial silicon layer on metallurgical silicon substrate.

Relative Atomic Fraction of Elements Deduced from SIMS Data

	As-Deposited Epitaxial Layer	Epitaxial Layer heated at 700°C for 12 hrs.	
		Grain	Grain Boundary
B			0.004
C	0.0035	0.003	0.005
Na	0.062	0.055	0.064
Mg	0.002	0.002	0.004
Al	0.003	0.001	0.004
Si	0.825	0.920	0.89
P	0.006	0.006	0.0098
K	0.092	0.010	0.01
Ca	0.005	0.005	0.009
Ti			0.0003
Cr	0.0003		0.0002
Mn	0.0004		0.0005
Fe			0.0004

Upon heat treatment in a helium atmosphere at 700°C for 12 hrs, the concentration of metallic impurities at grain boundaries, particularly magnesium, aluminum, calcium, titanium, chromium, manganese, and iron, are increased significantly (Table V). This precipitation of metallic impurities at grain boundaries is expected to improve the performance of epitaxial thin film solar cells.

V. Thin Film Silicon Solar Cells

Substrates prepared from the unidirectional solidification of aqua regia treated metallurgical silicon on graphite have been used for the fabrication of thin film solar cells. Since the substrate was of low resistivity p-type, the active region was prepared by the successive deposition of p- and n-type silicon films on the substrate using the thermal reduction of trichlorosilane containing appropriate dopants. Subsequent to the deposition process, the solar cell structures were heated in a helium atmosphere at 700°C to allow the diffusion of metallic impurities to grain boundaries. The graphite plate serves as the ohmic contact to the p-region. The grid contact was applied to the front surface of the cell by evaporating about 1000 \AA of titanium and $2\text{-}3\text{ }\mu\text{m}$ of silver to the cell surface through a metal mask, followed by annealing in a hydrogen atmosphere at 500°C . Anti-reflection coatings of tin oxide were applied by the oxidation of tetramethyltin in an argon atmosphere.

Nearly 100 large area solar cells (30 cm^2 or larger) have been produced during this period with the objective of investigating the effects of resistivity and thickness of the p- and n-regions on the photovoltaic characteristics of solar cells. In the first series of experiments, the thickness and resistivity of the surface n-region and the thickness of p-region were fixed: $2\text{ }\mu\text{m}$ of n-layer with carrier concentration graded from 10^{17} to 10^{20} cm^{-3} , and $20\text{ }\mu\text{m}$ of p-layer. The resistivity of the p-region was varied from 0.2 to 1 ohm-cm . At resistivities of 0.5 ohm-cm or higher, there was a definitive decrease in the open-circuit voltage and fill factor of the solar cells, due to the reduced contact potential across the p-n junction and the increased potential barriers across the grain boundaries. A p-layer resistivity of $0.2\text{-}0.3\text{ ohm-cm}$ appears to be optimum. In the second series of experiments, the thickness and resistivity of the n-region and the resistivity of the p-region

were fixed: 2 μm of n-layer with carrier concentration graded from 10^{17} to 10^{20} cm^{-3} , and a p-layer resistivity of 0.2 - 0.3 ohm-cm. The thickness of the p-region was varied from 10-30 μm . The photovoltaic characteristics of the solar cells, particularly the short-circuit current, were found to degrade significantly as the thickness of the p-region was reduced to 15 μm or less in thickness. Furthermore, no improvements were observed as the thickness of the p-region was increased to 25 μm or more, as expected from the diffusion length measurements. Thus, the thickness and resistivity of the p-region used in this program are near optimum for the n-region configuration selected.

The solar cell configuration discussed thus far, i.e., with a relatively thin n-region, is similar to the diffused solar cells. In such a configuration, the photocurrent is generated principally in the p-region. If the p-region has a relatively long minority carrier diffusion length, such as 100-200 μm , commonly observed in semiconductor grade single crystalline silicon, photogenerated carriers can be collected with good efficiencies. In epitaxial silicon films deposited on metallurgical silicon substrates, however, the diffusion length of minority carriers is only 15-20 μm , considerably smaller than the absorption length in silicon at wavelengths longer than about 0.9 μm . For example, the absorption length is approximately 45, 80, and 200 μm at wavelengths of 0.95, 1.0, and 1.05 μm , respectively. Thus, the collection of photogenerated carriers from the p-region alone will not be efficient, and the conversion efficiency will be relatively low. The collection efficiency can be increased if the contribution of photocurrent from the n-region can be significantly increased by increasing its thickness. This can be readily achieved by the epitaxial deposition technique. A number of solar cells have been prepared with the n-region 10-15 μm in thickness, and the photocurrent was found to increase by at least 10% for large area devices.

The solar cells prepared during this period are 30-60 cm^2 in area. The AM1 efficiency of 30-40 cm^2 solar cells is up to 9% and that of 60 cm^2 solar cells is slightly higher than 8%. Figure 4 shows the current-voltage characteristics of a 37 cm^2 area thin film silicon solar cell under illumination with quartz-halogen lamps at AM1 conditions. The open-circuit voltage, short-circuit current density, and fill factor are 0.57 V, 20.8 mA/cm^2 , and 75.6%, respectively, corresponding to an AM1 efficiency of 8.95%. Figure 5 shows the illuminated characteristics of a 60 cm^2 area solar cell with an AM1 efficiency of 8.3%.

The $\ln I_{sc}$ versus V_{oc} relation was used as a criterion to evaluate the quality of epitaxial junctions. Figure 6 shows such a relation for the 37 cm^2 area solar cell described above. The diode quality factor is nearly unity at voltages higher than about 0.5 V. In contrast with diffused cells, negligible shunting is observed at low voltages because of the large thickness of the n-region.

The spectral response of thin film polycrystalline silicon solar cells was measured at a set of discrete wavelengths selected by interference filters, and a calibrated single crystalline silicon solar cell of 4 cm^2 area was used as a reference. Figure 7 shows the spectral response of the solar cell in Figure 4 together with that of a calibrated cell for comparison. The peak response for the polycrystalline cell occurs at a shorter wavelength than that for the single crystalline cell. In addition, the quantum efficiency in the polycrystalline solar cell is lower than that in the single crystalline cell. The shift in peak response and lower quantum efficiency is not unexpected in view of the small thickness of the active region of, and the short minority carrier diffusion length in, the polycrystalline cell.

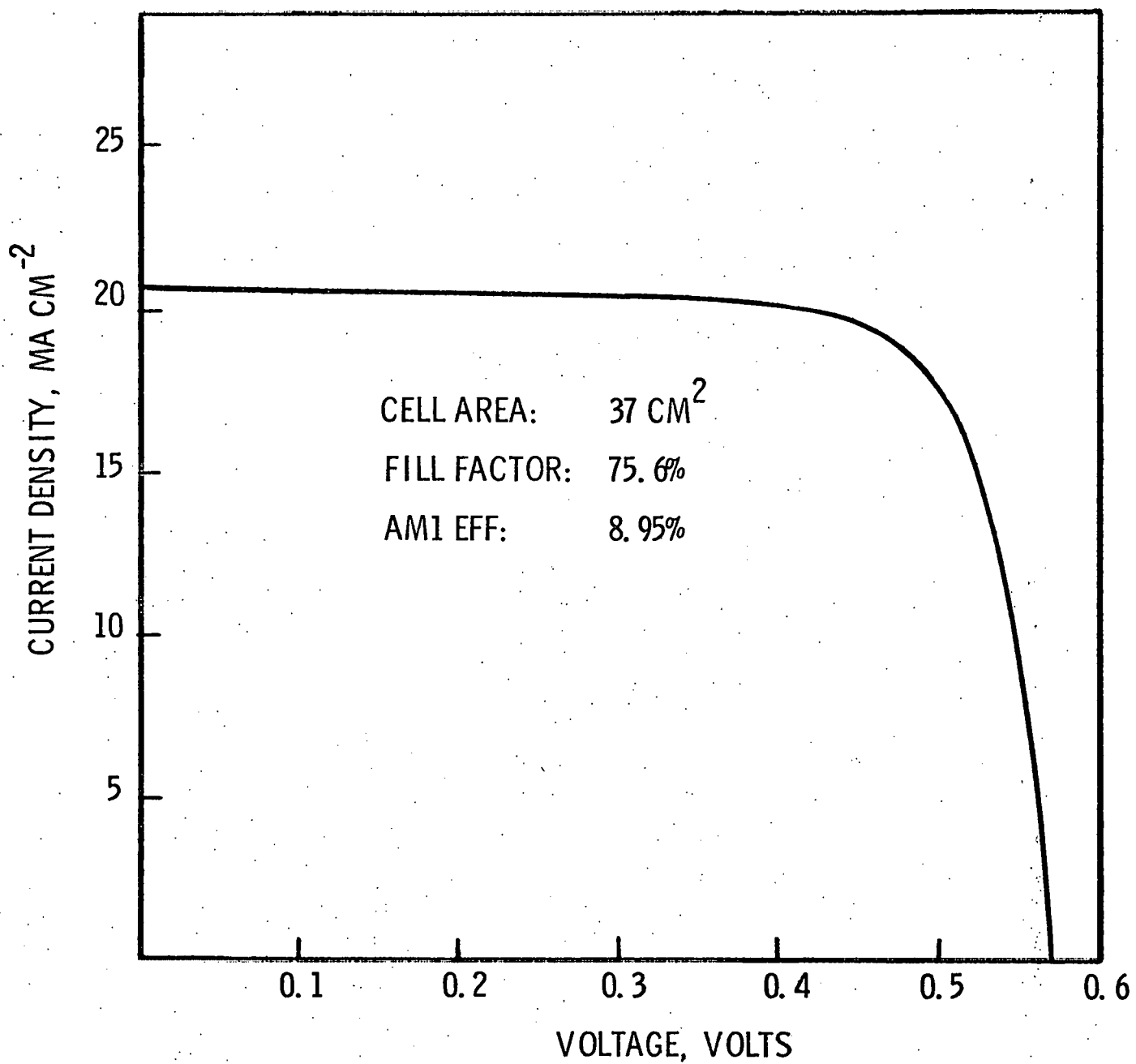


Figure 4 Current-voltage characteristics of a 37 cm² area polycrystalline thin film silicon solar cell under illumination with GE ELH quartz-halogen lamps equivalent to AM1 conditions.

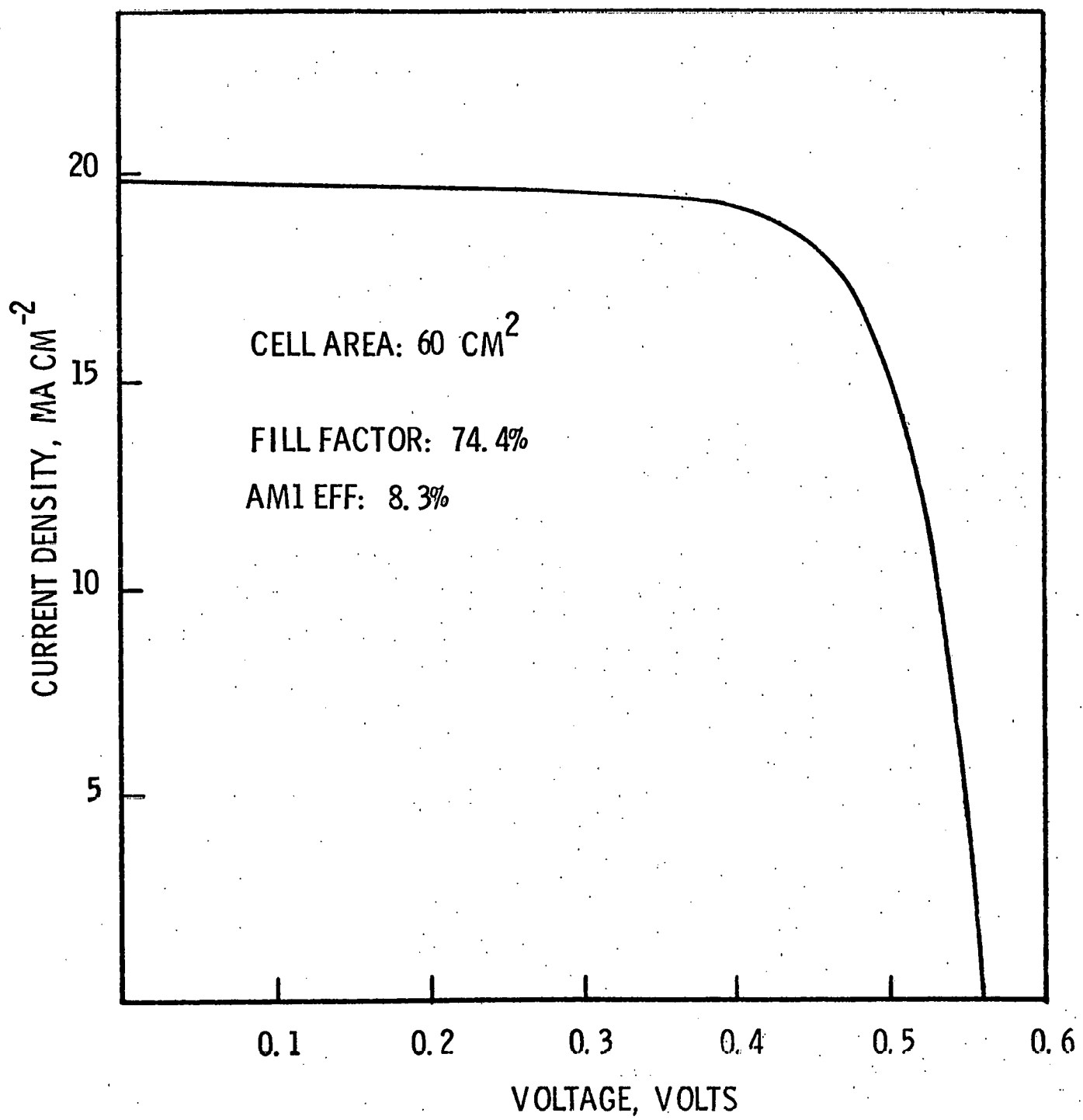


Figure 5 Current-voltage characteristics of a 60 cm^2 area polycrystalline thin film silicon solar cell under illumination with GE ELH quartz-halogen lamps equivalent to AM1 conditions.

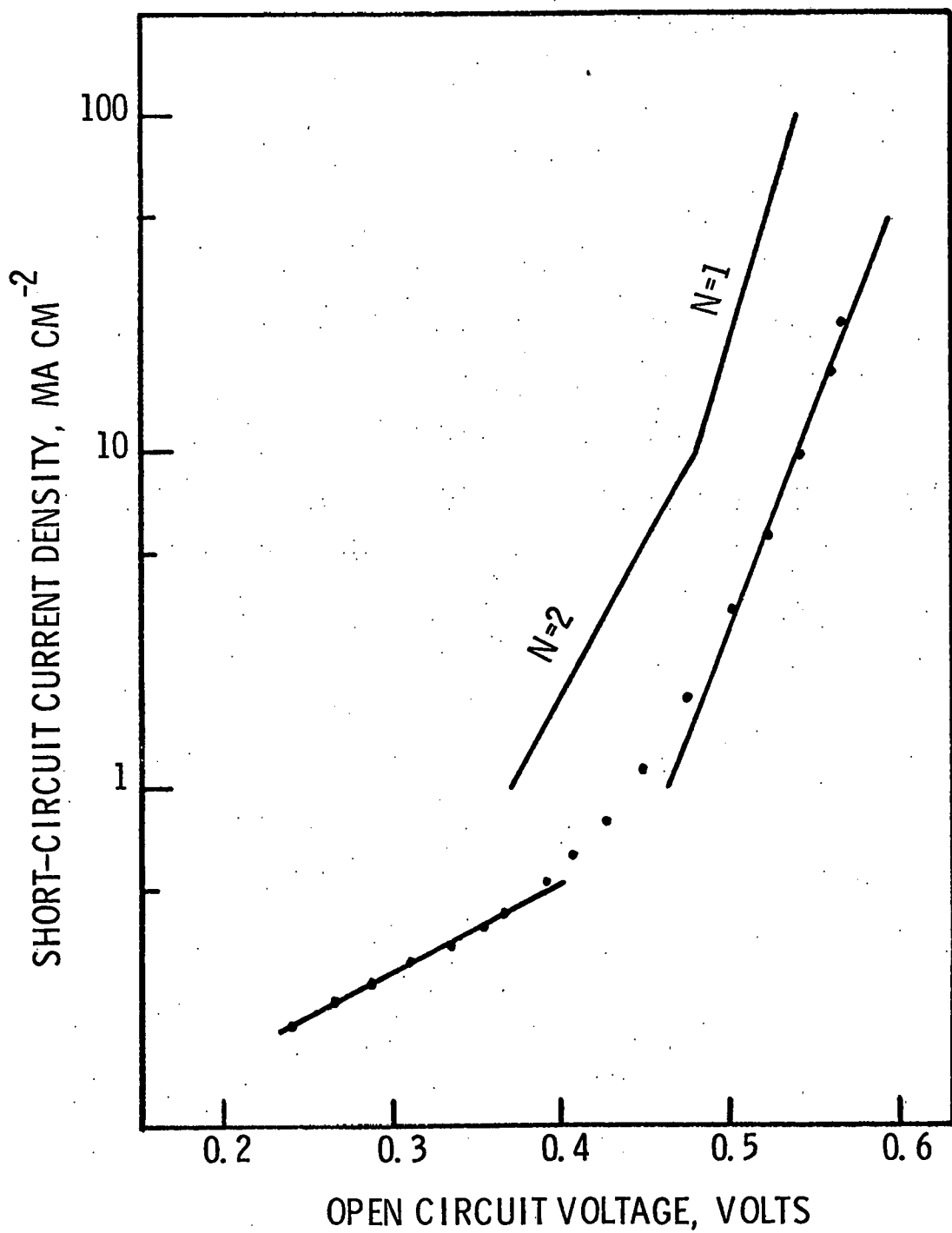


Figure 6 Short-circuit current and open circuit voltage relations of the thin film silicon solar cell shown in Fig. 4.

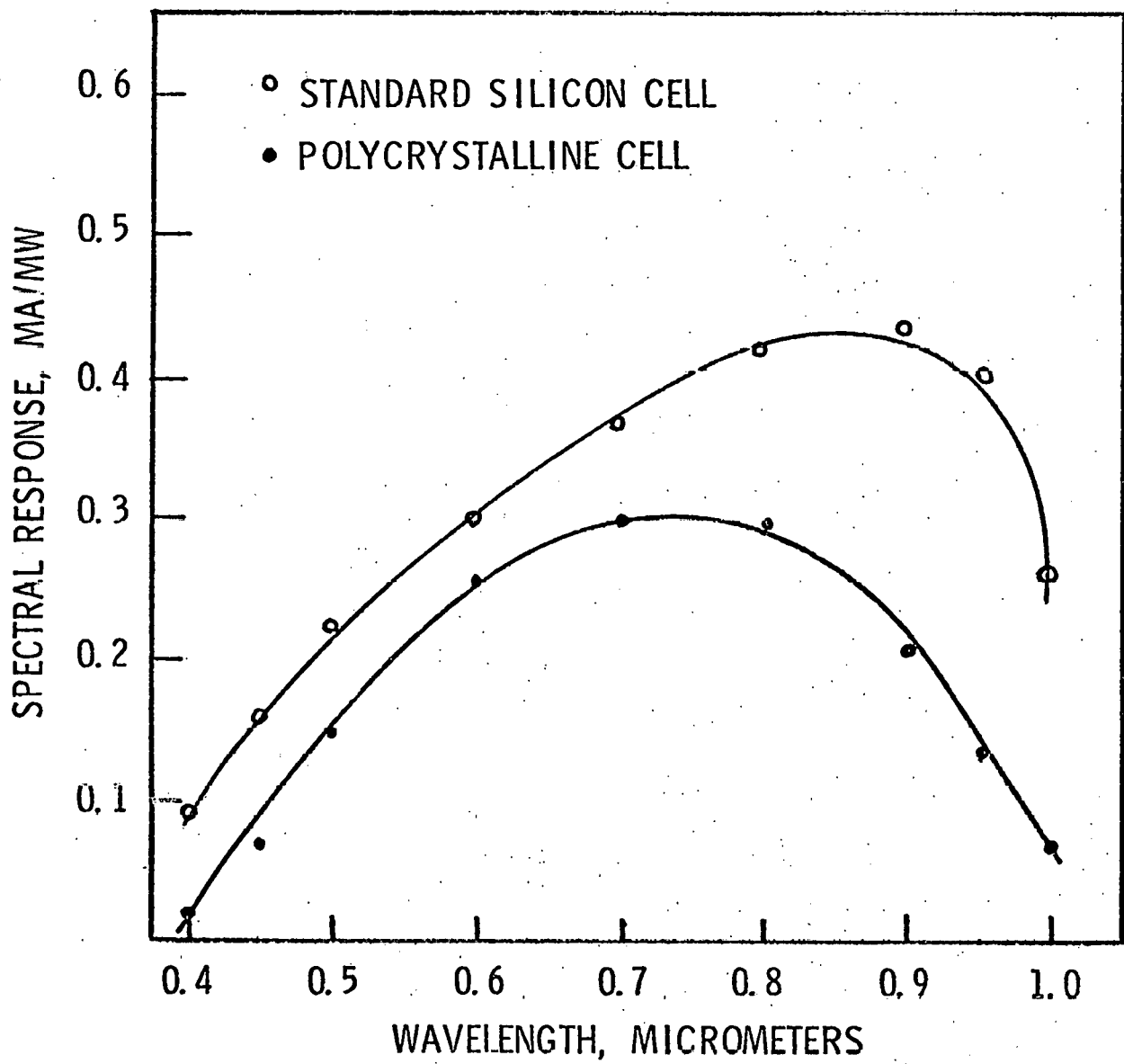


Figure 7 Spectral response of the thin film silicon solar cell shown in Figure 4.

VI. Plan for the Next Period

During the coming period, the conditions for the purification of metallurgical silicon by the acid-extraction technique will be optimized to further reduce the concentration of metallic impurities. The effects of the thickness and resistivity of the active region (epitaxial n- and p-layers) of the solar cell will be further investigated. The fabrication and characterization of solar cells will be continued.